

# Gauge Poisson representations for birth/death master equations

P. D. Drummond

Universität Erlangen-Nürnberg, Lehrstuhl für Optik, Staudstrasse 7/B2 D-91058 Erlangen, Germany.<sup>†</sup>

(Dated: 21st May 2019)

Poisson representation techniques provide a powerful method for mapping master equations for birth/death processes - found in many fields of physics, chemistry and biology - into more tractable stochastic differential equations. However, the usual expansion is not exact in the presence of boundary terms, which commonly occur when the differential equations are nonlinear. In this paper, a stochastic gauge technique is introduced that eliminates boundary terms, to give an exact representation as a weighted rate equation with stochastic terms. These methods provide novel techniques for calculating and understanding the effects of number correlations in systems that have a master equation description. As examples, correlations induced by strong mutations in genetics, and the astrophysical problem of molecule formation on microscopic grain surfaces are analyzed. Exact analytic results are obtained that can be compared with numerical simulations, demonstrating that stochastic gauge techniques can give exact results where standard Poisson expansions are not able to.

## I. INTRODUCTION

The calculation and prediction of the behavior of complex systems is one of the most pressing issues in theoretical physics[1]. A common problem when dealing with statistical problems is that the state-space of possible outcomes is enormous. This is particularly so for quantum systems - but very similar issues can arise in many types of master equation, with applications ranging from kinetic theory to genetics. One of the earliest approaches to this problem was the method of Langevin equations in Brownian motion, which led to the theory of equations with random terms, or stochastic equations. An important subsequent development in the field of discrete master equations was the van Kampen system-size expansion[2], which leads to an approximate Fokker-Planck equation equivalent to a stochastic equation, whose deterministic part has the usual rate-equation behavior. Following this, a more systematic technique was introduced, called the Poisson[3] expansion, which gives exact results in some cases with linear rate equations.

The general advantage of Poisson methods is that they employ a ‘natural’ basis, in which the distribution is expanded in the most entropically likely distribution for linear couplings. The disadvantage is that one may obtain large errors - both random and systematic - when nonlinear interactions act to generate sub-Poissonian variances. In this paper, a new method called the gauge Poisson representation is introduced, which allows an exact mapping of many important master equations into readily soluble stochastic differential equations, even when the Poisson expansion can not be used. It is the stochastic dynamics in these cases, and methods for treating them, that this paper is directed toward. As examples, I show how the gauge method can be used to calculate mean values and novel correlation predictions from master equations for genetic mutations in a simple model from

evolutionary biology[4], for the astrophysical problem of interstellar molecular hydrogen production on grain surfaces[5].

In master equations, the fundamental object is a probability distribution  $P(\mathbf{N}; t) = |\mathbf{P}(t)\rangle_{\mathbf{N}}$  for observing probabilities of discrete outcomes, labeled with integers  $\mathbf{N} = (N_1; \dots; N_d)$ . These numbers are typically the number of particles or atoms (in physics), molecules (in chemistry) or organisms (in biology)[1]. The numbers may refer to a large, well-mixed volume, or to cells within a larger volume in the case of spatially extended systems. A common and very significant problem is the Markovian time-evolution of the distribution, defined by an  $\mathbf{N} \times \mathbf{N}$  matrix  $\mathbf{M}$  so that:

$$\frac{\partial}{\partial t} \mathbf{P}(t) = \mathbf{M} \cdot \mathbf{P}(t) : \quad (1.1)$$

There are severe complexity issues that arise in trying to solve these equations as the number of dimensions increase. The difficulty of solving this equation directly is that the total number of states involved may grow exponentially large with the dimension or number of distinct modes  $d = \text{cells} \times \text{species}$ . Thus, direct methods are not suitable for solving many important problems of this type.

For large enough numbers  $N_j$ , one may use rate-equations or system-size expansions[1]. However, these approximations are inapplicable to many important problems where the actual numbers may be small in at least one of the steps. Examples of this are common in problems involving nano-structures - like the grains involved in astrophysical molecule production[5], where it is crucial to have more than one atom present for molecule formation. Other potential applications include genetic population dynamics[4], where population numbers in small regions are also critically important to reproduction, and spatially dependent master equations for diffusion or kinetic processes. Direct Monte-Carlo simulations can be used in these problems[6], but these can be inefficient and time-consuming for large numbers of modes, since they do not make any use of the fact that most of the populations involved may be nearly Poissonian.

A useful alternative is an exact expansion of the distribution vector  $\mathbf{P}$  using a continuous basis of ‘prototype’ solutions, namely the complex Poisson distribution  $\mathbf{p}_0(\boldsymbol{\alpha})$ , whose com-

Electronic address: drummond@physics.uq.edu.au; URL: [www.physics.uq.edu.au/BEC](http://www.physics.uq.edu.au/BEC)

<sup>†</sup>Permanent Address: Department of Physics, University of Queensland, QLD 4072, Brisbane, Australia

ponents are defined as:

$$[\mathbf{p}_0(\alpha)]_{\mathbf{N}} = \prod_{j=1}^d \frac{e^{-\alpha_j} (\alpha_j)^{N_j}}{N_j!} : \quad (1.2)$$

The usual Poisson representation[3] expands the distribution vector  $\mathbf{P}$  with a positive distribution of Poissonians,  $f(\alpha)$ , defined over a *complex*  $d$ -dimensional phase-space of variables  $\alpha$ . Here the discrete variable  $\mathbf{N}$  which is a vector of integers is transformed into a continuous variable  $\alpha$  which is a vector of complex numbers. This then can be used to transform the master equation given above into a stochastic differential equation, with just linear rather than exponential growth in the problem size, as the number of modes increases.

This transformation has similar properties to the positive-P[7] representation in quantum mechanics. It is exact if the resulting differential equation is linear, but there are subtleties when there are nonlinear terms in the equations. If unstable trajectories are generated[8] which cause the distribution to have power-law tails at large radius, then the resulting transformation develops systematic boundary term errors.

I show that the Poisson method can be modified using a stochastic gauge technique that stabilizes all complex trajectories that are already stable in the real phase-space. This absence of moving singularities is conjectured[9] to be sufficient to eliminate the boundary term errors, which will be verified in a typical example calculation. Thus, correctly chosen stochastic gauges appear to eliminate the boundary term problem, and simultaneously give rise to greatly reduced sampling errors in practical numerical solutions.

To illustrate the technique, I will consider examples in which there is relatively simple behavior that leads to sub-Poissonian results, in cases where there is an analytic theory available to compare with numerical simulations. This is used to demonstrate the accuracy and boundedness in some relatively extreme cases where boundary terms exist. In more typical applications, the correlations and fluctuations are closer to Poissonian, and the sampling error therefore would be smaller.

## II. GAUGE POISSON REPRESENTATION

The gauge Poisson representation introduced here treats the problem of boundary terms, by utilizing a gauge technique similar to that recently proposed for the positive-P distribution[10, 11]. It adds an extra variable to the distribution, which eliminates instabilities by modifying the dynamical equations. A type of gauge-invariance allows this to be carried out exactly. The resulting equations are almost identical to rate equations, except with stochastic terms. The gauge equations retain the advantages of the Poisson method, but have no boundary term errors for correctly chosen gauges. This is critically important for correct results where there are small numbers.

### A. Gauge phase-space expansion

The technical details are as follows. I define an extended (gauge) phase-space with  $\dot{\alpha} = (\Omega; \alpha)$ , and a renormalized Poisson distribution as  $\mathbf{p}(\dot{\alpha}) = \mathbf{p}_0(\alpha)\Omega$ . Here  $\Omega$  is a complex-valued weighting factor which weights (or multiplies) the usual normalized Poisson basis vector. The gauge expansion is defined for a real, positive distribution  $G(\dot{\alpha})$ , as:

$$\mathbf{P} = \int_{\dot{\alpha}}^{\mathbf{Z}} G(\dot{\alpha}) \mathbf{p}(\dot{\alpha}) d^d \dot{\alpha} : \quad (2.1)$$

I will show that this means that a freedom of choice becomes available in the equivalent stochastic equations. Importantly, it then is possible to choose an equivalent stochastic equation of motion without instabilities, which is conjectured to eliminate boundary terms. Hence, there is an exact mapping available, provided the propagation matrix  $\mathbf{M}$  can be constructed from a class of matrix ladder operators which either increase ( $\mathbf{L}_j^+$ ) the number of particles in a particular mode  $j$ , or decrease ( $\mathbf{L}_j^-$ ) the number of particles and multiply the probability by a factor of  $(N_j + 1)$ .

Explicitly, this means that:

$$\begin{aligned} \mathbf{L}_j^+ \mathbf{P} &= P(N_1; \dots; N_j - 1; \dots) \\ \mathbf{L}_j^- \mathbf{P} &= (N_j + 1)P(N_1; \dots; N_j + 1; \dots) : \end{aligned} \quad (2.2)$$

These ladder operators obey identities as follows, when acting on a Poisson distribution:

$$\begin{aligned} \mathbf{L}_j \mathbf{P} &= \alpha_j \mathbf{p}(\dot{\alpha}) \\ \mathbf{L}_j^+ \mathbf{P} &= (1 + \partial_j) \mathbf{p}(\dot{\alpha}) \\ \mathbf{p}(\dot{\alpha}) &= \Omega \partial_{\Omega} \mathbf{p}(\dot{\alpha}) : \end{aligned} \quad (2.3)$$

Since  $\mathbf{p}(\dot{\alpha})$  is analytic in  $\dot{\alpha}$ , I have used  $\partial = \partial_{\Omega} \partial_{\Omega} \dot{\alpha}$  to symbolize either  $\partial_j^x = \partial/\partial x_j$  or  $i \partial_j^y = \partial/\partial y_j$  for each of the  $j = 0; \dots; d$  complex variables  $\alpha_j = x_j + iy_j$ .

So far, this is similar to the positive Poisson representation[3]. However, the  $m$  th factorial moment is now given by a weighted average, with  $\Omega$  as a complex weighting parameter in the averages:

$$hN_j(N_j - 1) \dots (N_j - m) \mathbf{P} = \int_{\dot{\alpha}}^{\mathbf{Z}} \Omega \alpha_j^m G(\dot{\alpha}) d^d \dot{\alpha} : \quad (2.4)$$

From this one obtains the expected result that in a pure Poisson distribution,  $G(\dot{\alpha}) = \delta(\dot{\alpha} - \bar{\alpha}) \prod_{j=1}^d \delta(\alpha_j - \bar{\alpha}_j)$ , the mean and variance of modes with  $j > 0$  are given by:

$$\begin{aligned} hN_j i &= \bar{\alpha}_j \\ h(N_j - \bar{N}_j)^2 i &= \bar{\alpha}_j : \end{aligned} \quad (2.5)$$

## B. Poisson Fokker-Planck Equation

Using the operator identities given above, the operator equations can always be transformed to an integro-differential equation of form:

$$\frac{\partial}{\partial t} \mathbf{P}(t) = \overset{Z}{G}(\dot{\alpha}) \mathcal{L}_A \mathbf{p}(\dot{\alpha}) d^{2(d+1)} \dot{\alpha} ; \quad (2.6)$$

where the notation  $\mathcal{L}_A$  indicates an ordering of all derivative operators to the right. In order to demonstrate this, consider a generic binary interaction, in which two species are transformed at a rate  $k$  into two new species:

$$X_1 + X_2 \xrightarrow{k} X_3 + X_4 : \quad (2.7)$$

Introducing  $N_j = N_j - 1$ , the master equation is:

$$\frac{\partial}{\partial t} P(\mathbf{N}) = k (N_1^+) (N_2^+) P(N_1^+; N_2^+; N_3; N_4) - k N_1 N_2 P(\mathbf{N}) : \quad (2.8)$$

This can also be represented using matrices as:

$$\frac{\partial}{\partial t} \mathbf{P} = k \mathbf{L}_3^+ \mathbf{L}_4^+ - \mathbf{L}_1^+ \mathbf{L}_2^+ \mathbf{L}_1 \mathbf{L}_2 \mathbf{P} : \quad (2.9)$$

Hence, in this case:

$$\begin{aligned} \mathcal{L}_A &= k \alpha_1 \alpha_2 [(1 + \partial_3) (1 + \partial_4) - (1 + \partial_1) (1 + \partial_2)] \\ &= k \alpha_1 \alpha_2 [\partial_3 + \partial_4 - \partial_1 - \partial_2 + \partial_3 \partial_4 - \partial_1 \partial_2] : \end{aligned} \quad (2.10)$$

It follows that in cases of interest involving at most binary kinetics, only first and second order derivatives occur, giving a differential operator in the form:

$$\mathcal{L}_A = A_j^+ \partial_j + \frac{1}{2} D_{ij} \partial_i \partial_j : \quad (2.11)$$

Here the repeated Latin indices  $i, j$  are summed over  $i = 1 \dots d$ , so that  $A_j^+$  is a  $d$ -component complex vector identical to the usual Poisson representation drift, while  $D_{ij}$  is a  $d \times d$  square complex matrix. As a first step towards obtaining stochastic equations, it is useful to take a  $d \times d$  matrix square root  $\mathbf{B}$ , where  $\mathbf{D} = \mathbf{B} \mathbf{B}^T$ . It should be noted that this is a non-unique choice. The lack of uniqueness of matrix square-roots allows arbitrary functions in phase-space to be introduced at this stage, which can be thought of as a diffusion gauge. However, these cannot stabilize trajectories with deterministic moving singularities.

The standard procedure of the positive Poisson representation would then be to use partial integration to obtain a Fokker-Planck differential operator acting on the distribution  $G$ , which is then transformed into a stochastic differential equation using the dimension-doubling technique described in more detail in the next section. In the present example, this procedure - which is only valid if boundary terms vanish during the partial integration - would result in a stochastic

equation for the complex Poisson mean variables  $\alpha_j$ . On introducing a complex ‘reaction rate’,  $R = k\alpha_1 \alpha_2$ , the result is:

$$\begin{aligned} \frac{d\alpha_1}{dt} &= R + \overset{P}{\int} \frac{R}{R=2} (\zeta_1 + i\zeta_2) \\ \frac{d\alpha_2}{dt} &= R + \overset{P}{\int} \frac{R}{R=2} (\zeta_1 - i\zeta_2) \\ \frac{d\alpha_3}{dt} &= R + \overset{P}{\int} \frac{R}{R=2} (\zeta_3 + i\zeta_4) \\ \frac{d\alpha_4}{dt} &= R + \overset{P}{\int} \frac{R}{R=2} (\zeta_3 - i\zeta_4) ; \end{aligned} \quad (2.12)$$

This shows very clearly a useful property of the Poisson method. The modified particle statistics caused by nonlinear reactions are immediately apparent from the noise terms, since any fluctuations represent a departure from Poisson statistics. The difficulty with the standard[3] positive Poisson method outlined above is that even normally stable kinetic equations can become unstable due to moving singularities in this extended complex phase-space. While the singular trajectories form a set of measure zero, they lead to Fokker-Planck equations with power-law tails that do not vanish sufficiently quickly at the phase-space boundaries[9].

In the present example, the singular trajectories occur at negative values of  $\alpha_{1,2}$ , which can be reached via stochastic motion in the complex plane. The resulting moving singularity in the deterministic equations is of form  $1 = \alpha_1 = 1 = \alpha_2 = k(t - t_0)$  for  $t < t_0$ . Moving singularities like this one often exist in complex nonlinear equations of polynomial form, since these systems are generically non-integrable or even chaotic - and the Painleve conjecture[12] states that moving singularities are to be expected in analytically continued non-integrable sets of equations. This means that in many cases, the boundary terms do not vanish, leading to systematic errors. Although such errors are known to be exponentially small when there is large linear damping, they can cause problems when there is little or no linear damping.

## III. GAUGE IDENTITIES

Fortunately, the extra variable  $\Omega$  allows the  $\partial_0$  differential identity to be used to introduce a *stochastic gauge* - an arbitrary vector function in the extended phase-space with  $d + 1$  complex dimensions. This can be used to stabilize the drift equations throughout the extended phase-space, thus allowing integration by parts. There is no free lunch here, however! The price that is paid is a new stochastic noise term, leading to a finite variance in the gauge amplitude  $\Omega$ . While this can cause practical problems due to sampling errors - which must be minimized - it is important to note that these errors can be estimated and controlled by choice of gauge and by increasing the number of sample trajectories. By contrast, there is no presently known technique of estimating and controlling boundary term errors in the standard Poisson expansion.

### A. Gauge Fokker-Planck Equation

To demonstrate the stochastic gauge technique, I now introduce  $d$  arbitrary complex functions  $\mathbf{g} = (g_i(\alpha; t))$ , to give a new differential operator  $\mathcal{L}_G$  which is equivalent to  $\mathcal{L}_A$ , but which includes  $\Omega$  derivatives in the extended phase-space:

$$\mathcal{L}_G = \mathcal{L}_A + \frac{1}{2} \mathbf{g} \Omega \partial + \sum_{k,j=1}^d g_k B_{jk} \partial_j \Omega \partial_\Omega - 1 : \quad (3.1)$$

This will later be transformed, using the choice of analytic derivatives, into a positive definite Fokker-Planck equation.

Summing repeated Latin indices from now on over  $i = 0; d$ , this becomes:

$$\mathcal{L}_G = A_i \partial_j + \frac{1}{2} D_{ij} \partial_i \partial_j : \quad (3.2)$$

Here, the *total* complex drift vector, including gauge corrections, is  $\mathbf{A} = (0; A_1; \dots; A_d)$ , where:

$$A_j = A_j^+ - g B_{jk} [j; k > 0] : \quad (3.3)$$

This remarkable result shows that as long as there is a non-vanishing noise or  $B_{jk}$  term, the drift equation can be modified in an arbitrary way by adding the gauge term  $-g B_{jk}$ .

But this is not without a price, since the diffusion matrix has changed as well. The total diffusion matrix  $\underline{\underline{D}}$  is a  $(d+1) \times (d+1)$  matrix, with a new  $(d+1) \times d$  square root  $\underline{\underline{B}}$ :

$$\begin{aligned} \underline{\underline{D}} &= \Omega^2 \mathbf{g} \mathbf{g}^T; \Omega \mathbf{g} \mathbf{B}^T \\ &= \mathbf{B} \mathbf{g}^T \Omega; \mathbf{B} \mathbf{B}^T \\ &= \frac{\Omega \mathbf{g}}{\mathbf{B}} \frac{\Omega \mathbf{g}^T}{\mathbf{B}^T} \mathbf{B}^T = \underline{\underline{B}} \underline{\underline{B}}^T : \end{aligned} \quad (3.4)$$

Thus, the  $(d+1) \times d$  complex stochastic noise matrix  $\underline{\underline{B}}$  is as before, except with one added row:

$$\underline{\underline{B}} = \frac{\Omega \mathbf{g}}{\mathbf{B}} : \quad (3.5)$$

The additional row means that whenever a gauge term is added, a corresponding noise term appears in the equation of motion for the gauge amplitude variable  $\Omega$ . The details of this are derived next.

### B. Stochastic equations

So far, there is no restriction on which of the choices of analytic derivative is utilized to obtain the identities. This means that it is possible to use the free choice of equivalent identities to give a differential operator which is entirely real and has a positive-definite diffusion. This procedure is also followed in the positive P[7] and positive Poisson[3] representations. Here it is extended[11] to include the gauge variable  $\Omega$  as well as the other variables. This is achieved by introducing a  $2(d+1)$

dimensional real phase space  $(x_0; \dots; x_d; y_0; \dots; y_d)$ , with derivatives  $\partial_\mu$ . Next, divide  $\underline{\underline{B}} = \underline{\underline{B}}^x + i \underline{\underline{B}}^y$  into its real and imaginary parts. A similar procedure is followed for  $\underline{\underline{A}} = \underline{\underline{A}}^x + i \underline{\underline{A}}^y$ .

The choice for the analytic derivative, where  $\partial_j = \partial_i^x + i \partial_i^y$ , can now be made definite by choosing it so the resulting drift and diffusion terms are always real. In more detail, this corresponds to choosing:

$$\begin{aligned} A_i \partial_i &= A_i^x \partial_i^x + A_i^y \partial_i^y ; \\ D_{ij} \partial_i \partial_j &= B_{ik}^x B_{jk}^x \partial_i^x \partial_j^x + B_{ik}^y B_{jk}^y \partial_i^y \partial_j^y + (x \neq y) : \end{aligned} \quad (3.6)$$

At this point, it is necessary to introduce a corresponding real drift vector  $\mathcal{A}_\mu$  and diffusion matrix  $\mathcal{D}_{\mu\nu}$  which are defined on the  $2(d+1)$  dimensional real phase space. Hence, the gauge differential operator can now be written explicitly in this equivalent real form, as:

$$\mathcal{L}_G = \mathcal{A}_\mu \partial_\mu + \frac{1}{2} \mathcal{D}_{\mu\nu} \partial_\mu \partial_\nu ; \quad (3.7)$$

where  $\underline{\underline{D}} = \underline{\underline{B}} \underline{\underline{B}}^T$  is now positive semi-definite. This can be seen by writing  $\underline{\underline{B}}$  as a  $2(d+1) \times d$  real matrix:

$$\underline{\underline{B}} = \begin{pmatrix} \underline{\underline{B}}^x \\ \underline{\underline{B}}^y \end{pmatrix} ; \quad (3.8)$$

so that the diffusion matrix is the square of a real matrix, with:

$$\underline{\underline{D}} = \begin{pmatrix} \underline{\underline{B}}^x & \mathbf{h} \\ \mathbf{h}^T & \underline{\underline{B}}^x \end{pmatrix} ; \quad (3.9)$$

Thus, by choosing the analytic derivatives to give real terms in  $\mathcal{L}_G$ , with a positive semi-definite diffusion operator on a real space of  $2(d+1)$  dimensions is obtained. The full evolution equation is then:

$$\frac{\partial}{\partial t} \mathbf{P}(t) = \begin{pmatrix} \mathbf{Z} \\ G(\alpha) \mathcal{L}_G \mathbf{P}(\alpha) \end{pmatrix} d^{2(d+1)} \alpha : \quad (3.10)$$

Provided that one can integrate by parts, there is at least one solution for  $G$  which satisfies the positive-definite Fokker-Planck equation:

$$\frac{\partial}{\partial t} G(\alpha; t) = \partial_\mu \mathcal{A}_\mu + \frac{1}{2} \partial_\mu \partial_\nu \mathcal{D}_{\mu\nu} G(\alpha; t) : \quad (3.11)$$

It is important to note here that the crucial partial integration step is only permissible if the distribution is strongly enough bounded at infinity ( $|\alpha| \rightarrow \infty$ ) so that all boundary terms vanish. Typically this means that the distribution must be bounded more strongly than all power laws in  $1=|\alpha|$ .

The positive-definiteness of the diffusion matrix  $\underline{\underline{D}}$  then implies that the Fokker-Planck equation is equivalent to a set of  $d+1$  Ito stochastic differential equations, with  $d^0$  real Gaussian processes  $\zeta_i(t)$ . This central result can be written compactly using the complex variable form, as:

$$\begin{aligned} \frac{d\Omega}{dt} &= \Omega \sum_{k=1}^{d^0} g_k \zeta_k(t) ; \\ \frac{d\alpha_j}{dt} &= A_j^+ (\alpha) + \sum_{k=1}^{d^0} B_{jk} \zeta_k(t) - g_k : \end{aligned} \quad (3.12)$$

The noises  $\zeta_i$  have correlations  $\langle \zeta_i(t) \zeta_j(t^0) \rangle = \delta_{ij} \delta(t - t^0)$ , and are uncorrelated between time steps.

#### IV. STABILIZING GAUGES

It is crucial at this stage to choose  $\mathbf{g}$  so that the resulting dynamics are not singular. No deterministic trajectory can be allowed to reach the boundary in a finite time, even on a set of initial conditions with measure zero, as this is the signature[9] for a distribution with a power-law tail - which cannot be integrated by parts exactly. This is an important question of principle, as it can lead to systematic errors.

A second criterion of practical significance, is to use a gauge that does not alter trajectories in the most probable and stable regions. If this is not satisfied, then the stochastic noise in the gauge amplitude  $\Omega$  creates a relatively large and growing sampling error. It should be realized that this is not an issue of mathematics, but rather one of computational efficiency. In performing a numerical calculation, there are always some numerical errors. These are due to the finite nature of computers (and even human calculators). Thus, one has to estimate and minimize numerical errors due to round-off error, finite step-size in time, and sampling error due to the use of a finite sample of trajectories.

In general, there is an optimum gauge which minimizes sampling errors, but even a non-optimal gauge can be used simply by increasing the number of sampled trajectories. In this section, I demonstrate the existence of stabilizing gauges. In the following sections, the numerical simulation of a realistic nonlinear master equation (which generates boundary term errors without a stabilizing gauge) is shown to give correct results within the sampling error. The important issue, as always, is that the calculated result must agree with the correct value within a known error-bar.

##### A. General master equation

The most general case considered here consists of a number of coupled reactions, labeled with an index  $r$ . Each reaction has the following generic structure:

$$\sum_j v_j^r X_j \xrightarrow{k^r} \sum_j \mu_j^r X_j : \quad (4.1)$$

Here the reactions are restricted to be at most binary, so that  $\mu_j^r; v_j^r = 0; 1; 2$ , and  $\sum_j \mu_j^r; \sum_j v_j^r = 2$ . Using the identities of Eq (2.3) the following Fokker-Planck equations are found, with a similar pattern to the previous example, Eq (2.10):

$$\frac{\partial G(\mathbf{n})}{\partial t} = \sum_r \left( \prod_j (1 - \partial_j)^{\mu_j^r} \prod_j (1 + \partial_j)^{v_j^r} \right) k^r \prod_j \alpha_j^{v_j^r} G(\mathbf{n}) : \quad (4.2)$$

This is transformed into a stochastic gauge equation by first introducing a reaction rate  $R^r$  for the  $r$  th reaction:

$$R^r = k^r \prod_j \alpha_j^{v_j^r} :$$

With this definition, the basic drift and noise matrices of the gauge stochastic differential equations, Eq (3.12) are given by a result of Gardiner[3], on considering all possible values and combinations of  $\mu_j^r; v_j^r$ :

$$\begin{aligned} A_j^+ &= \sum_r \mu_j^r v_j^r R^r \\ D_{ij} &= \sum_r R^r \mu_i^r \mu_j^r (\delta_{ij} - v_i^r v_j^r \delta_{ij}) \\ &= \sum_k B_{ik} B_{kj} : \end{aligned}$$

##### B. Minimal gauge selection

Just as in the simpler example of Eq (2.10), these equations only have constant, linear and quadratic terms. Hence, the unmodified drift equation for the  $a$ -th component can always be written as:

$$\frac{\partial \alpha_i}{\partial t} = C_i + \sum_j L_{ij} \alpha_j - \sum_j Q_{ij} \alpha_i \alpha_j + \sum_{jk} Q_{ijk}^+ \alpha_j \alpha_k ; \quad (4.3)$$

where all coefficients are real, and the quadratic terms are defined as positive:  $Q^+ > 0, Q > 0$ . Note that the structure of the kinetic equations is such that creation terms  $Q_{ijk}^+$  may involve any of the numbers  $\alpha_j; \alpha_k$ ; while the annihilation terms  $Q_{ij}$  have to involve least one number  $\alpha_i$  which has the same index as on the left hand side.

I now wish to demonstrate that there is a minimal stabilizing gauge, provided that the following conditions are satisfied:

the deterministic rate equations are stable even with linear terms removed

linear terms introduce no new instabilities to the gauge equations

This proof gives only minimal conditions for gauge-stabilization. Other stable gauges also exist, and may be more efficient in terms of sampling error in any given case.

Any deterministic instability is generally ruled by various conservation laws *a priori*. The present equations are not always strictly number-conserving however - i.e., reservoirs are allowed. Nevertheless, I assume them deterministically stable, in the sense of having no moving singularities for any positive real values of  $\alpha_j$ , even without linear terms. Certainly, if finite time singularities occur in a rate equation solution, then the nonlinear terms in the master equation are necessarily unphysical. Note that moving singularities *only* occur when there are nonlinear terms, so the addition or removal of linear terms is usually not crucial.

A moving singularity can occur in the analytic continuation of the rate equations, which are the precise equations found in

the usual positive Poisson equations. It is essential to remove any singularities if the resulting stochastic equations are to be accurate and useful - although the equations with singularities can still be used as approximate equations for large particle number.

Since the Painleve conjecture[12] states that moving singularities are a generic property of non-integrable sets of equations, it is to be expected that these will generally occur. Each singularity has the signature that for at least one component  $j$ , it evolves to  $\dot{\alpha}_j \rightarrow \infty$  in a finite time  $t_0$ , and hence must typically have a leading term with an inverse power-law time-dependence with power  $p_j$  for  $t < t_0$ :

$$\alpha_j = \frac{\alpha_j^0}{t_0 - t^{\gamma_j}} : \quad (4.4)$$

Several different power laws are possible on a given trajectory, depending on the species  $j$ . Suppose there is already a singularity in the complex nonlinear rate equations with linear terms set to zero. Since constant terms have a zero power, the singularity must also exist in a reduced set of equations, with leading terms at most of form:

$$\frac{\partial \alpha_i}{\partial t} = \sum_{j,k} Q_{ijk}^+ \alpha_j \alpha_k - \sum_j Q_{ij} \alpha_i \alpha_j : \quad (4.5)$$

Therefore, the leading terms in each singular equation have power laws and amplitudes of form satisfying:

$$\begin{aligned} p_i + 1 &= p_j + p_k = p_i + p_j \\ p_i \alpha_i^0 &= Q_{ijk}^+ \alpha_j^0 \alpha_k^0 - Q_{ij} \alpha_i^0 \alpha_j^0 : \end{aligned} \quad (4.6)$$

In this equation, only those terms whose powers match the LHS have to be included.

### 1. Circular gauge

Next, it is important to choose an appropriate diffusion gauge - that is, the choice of matrix square root of the diffusion matrix must be specified. This is most simply done by choosing to regard each distinct unidirectional reaction as having a distinct noise term - proportional to the reaction rate  $R^r$ . This choice may not always be optimal for sampling purposes, but it is a possible choice, and there is a resulting drift gauge which is stable.

This follows, since every nonlinear rate equation of form  $d\alpha/dt = R \propto \alpha_i \alpha_j = \sqrt{R} \alpha_i \alpha_j \exp(\phi_j + \phi_k)$  has a corresponding noise proportional to  $\sqrt{R}$ . Thus, it is always possible to subtract the gauge term

$$gB = R [1 \exp(i(\phi_j + \phi_k))] : \quad (4.7)$$

which cancels the original rate and replaces it by one rotated by a phase angle  $\phi$  equal to the phase of  $\alpha$ . The deterministic part of such an equation can only modify the amplitude of  $\alpha$ , and so is effectively restricted to a one-dimensional real space, just as the usual rate equations are.

The gauge-modified equation is non-analytic, and should have no Painleve type singularities, because all phases match. This is easily demonstrated from the fact that any singular solution must satisfy Eq (4.6) with all  $\alpha_j^0$  real and positive. But this would give rise to a singularity in the corresponding nonlinear deterministic rate equations, which is ruled out by hypothesis. The process can be iterated until all singularities are removed.

Hence, the gauge corrected equations with only nonlinear terms are stable. This implies stability in the complete set - provided the linear terms can introduce no new instabilities, as was assumed. When the rate-equations have an attractor, this gauge tends to produce random circular paths instead of localized behavior in the complex phase-space. I will therefore refer to it as the 'circular' gauge.

### 2. Phase gauge

The circular gauge can be further improved by modifying the gauge term so that it also stabilizes the phase near  $\phi = 0$ . This reduces the size of the gauge-induced noise, and hence reduces sampling errors. A suitable choice is:

$$gB = R [1 \exp(i(\phi_j + \phi_k))] : \quad (4.8)$$

Here the real part of  $f(\phi)$  satisfies  $\Re f(\phi) = 1$ ; while the imaginary part has an attractor at  $\phi = 0$ , where the gauge correction is defined to vanish. An example of this, treated in more detail later, is when  $R = \sqrt{R}$ . In this case, one can simply choose:

$$gB = n [1 \exp(i(\phi_j + \phi_k))] = R [1 \exp(i(\phi_j + \phi_k))] : \quad (4.9)$$

This has no effect on global stability, but increases the likelihood of trajectories near  $\phi = 0$ , where the phase gauge above generates a deterministic equation in the form  $d\phi/dt \propto \phi$ .

Since the most likely trajectory is in-phase and has zero gauge correction, the corresponding gauge noise and resulting sampling errors are reduced, as I will show later in the numerical examples. This gauge will be called the 'phase' gauge, as it stabilizes the phase-angle of  $\alpha$  as well as the modulus.

## C. Numerical Simulations

The results of direct numerical simulations can be used to test the necessity and effectiveness of different stochastic gauges. The numerical results included in this paper are simple examples where the detailed results of simulations can be evaluated in exactly soluble cases. In particular, it is important to verify (in at least some cases) that gauges with no moving singularities lead to exact simulations - without the systematic boundary term errors of the Poisson method. Although similar nonlinearities occur in spatially extended systems[13], more subtle gauge choices may be better in these cases.

### 1. Stratonovic calculus

Stochastic calculus is normally carried out in one of two different forms. The first is the Ito calculus, where all terms that multiply a stochastic noise are evaluated before carrying out the stochastic step forward in time. This is the simplest form, and corresponds directly to the coefficients in the type of Fokker-Planck equation used in the earlier sections of this paper. The second is the Stratonovic form, where all the multiplicative terms are evaluated implicitly at the midpoint of a given step forward in time. This form corresponds to taking the wide-band limit of a finite band-width stochastic equation, and follows more standard calculus rules for variable-changes.

For numerical simulations[14] it is generally more efficient to use Stratonovic equations[3] - in which the Ito drift term is modified in a standard way to allow central difference algorithms to be employed. In a generic Ito equation with coefficients corresponding to those in the real Fokker-Planck equation of Eq (3.11), the Stratonovic method generates a modified drift term  $\mathcal{A}_\mu^s$ , where:

$$\mathcal{A}_\mu^s = \mathcal{A}_\mu - \frac{1}{2} \mathcal{B}_{\mu\nu} \partial_\mu \mathcal{B}_{\mu\nu} : \quad (4.10)$$

The resulting equations can be used directly in stable implicit central-difference algorithms, which are robust and well-suited to the present nonlinear equations.

### 2. Error estimation

Discretization error can be estimated by comparing simulations with different step-sizes, but identical underlying noise sources. The maximum discretization error was typically of order  $10^{-3}$  in the simulations in this paper. The algorithm used was an iterative implicit central difference method[14], which directly implements the Stratonovic form of the stochastic equation. All numerical code was generated in C++ including estimators of both the sampling error and discretization error, using an XML script and an automatic code generator[15] obtained from the XMDS project website.

As an estimator of sampling error, I use the Gaussian estimator of the standard deviation in the mean,  $\sigma_m = \sigma = \sqrt{\frac{1}{N_s}}$ . However, it should be noted that more sophisticated estimators may be needed when the results are strongly non-Gaussian, as in some of the Poisson simulations.

To ensure that the results were a strong test of the stochastic gauge method, a large number of  $N_s = 10^6$  samples were used, to give low sampling errors  $\sigma_m$ .

## V. GENETIC MUTATION MASTER EQUATION

As one example, first consider the genetic problem of a stochastic master equation for a finite population, in which case the  $N_j$  are simply the populations of genotype  $j$ . A simple model for linear evolution through asexual reproduction

and mutation is of the form[4]:

$$\begin{aligned} X_j &\stackrel{!}{=} k_j 0 \\ X_i &\stackrel{!}{=} k_{ij} X_i + X_j : \end{aligned} \quad (5.1)$$

Here  $k_{ii} = (1 - Q)k_i^b$ , where  $k_i^b = \sum_j k_{ij}$  is the total birth rate,  $k_i$  is the death rate, and  $Q_i$  is the mutation rate. Defining  $\mathbf{N} \stackrel{!}{=} [N_1; N_2; \dots; N_l]$ , the corresponding master equation is:

$$\begin{aligned} \frac{d}{dt} P(\mathbf{N}) &= \sum_{i;j} k_{ij} N_i + \sum_i k_i N_i P(\mathbf{N}) \\ &+ \sum_i k_i (N_i + 1) P(\mathbf{N}^+ \stackrel{!}{=} ) \\ &+ \sum_{i;j} k_{ij} (N_j - 1) P(\mathbf{N} \stackrel{!}{=} [j]) : \end{aligned} \quad (5.2)$$

This has well-known problems: the state-space may be very large, preventing a direct matrix solution. On the other hand, while the corresponding average rate-equations reduce to the widely-studied Eigen[4] quasi-species model, the rate-equations are unable to treat population fluctuations in small samples.

### A. Stochastic equations

The equivalent Poissonian stochastic equation is exact for the problem given here, *without requiring a system-size expansion*. It is:

$$\frac{d\alpha_j}{dt} = -k_j \alpha_j + \sum_i k_{ij} \alpha_i + B_{jk} \zeta_k(t) : \quad (5.3)$$

Here, the noise matrix  $B_{jk}$  is determined from the symmetrized diffusion matrix,  $D_{ij} = [\alpha_i k_{ij} + \alpha_j k_{ji}]$  where:

$$\sum_k B_{ik} B_{jk} = D_{ij} : \quad (5.4)$$

This tells us immediately an important result: an initially Poissonian distribution is invariant under pure decay processes, but can develop increased fluctuations with non-Poissonian features due to birth and mutation events. In general, constructing the square root of a symmetric real matrix  $D_{ij}$  is non-unique. The most powerful technique requires a matrix diagonalization through an orthogonal transformation, and may result in eigenvalues of either sign. If all the eigenvalues are positive, the resulting fluctuations are super-Poissonian. If some are negative, at least one sub-Poissonian feature will occur, and a complex stochastic process will result.

A simple, even though somewhat extreme, example is obtained by considering a symmetric two-species case with  $Q_j = 1$ ,  $k = k_j$ ,  $k_m = k_{12}$  - so that mutations always occur. In this (rather unrealistic) case, the diffusion is entirely off-diagonal, and the Poisson representation exactly transforms an exponentially complex master equation into a soluble stochastic equation. This can be simplified further as follows, on introducing

$n_+ = (\alpha_1 - \alpha_2)$  and  $k = (k - k_m)$ :

$$\begin{aligned}\frac{dn_+}{dt} &= k n_+ + \frac{p}{2k_m n_+} \zeta_1(t) \\ \frac{dn}{dt} &= k^* n + i \frac{p}{2k_m n_+} \zeta_2(t) : \quad (5.5)\end{aligned}$$

In this situation, there is an absorber at  $n_+ = 0$ , since any stochastic trajectory that reaches this value has a zero derivative. This is due to the randomness of birth or death events, which mean that it is always possible for the random walk in this low-dimensional population space to finish at extinction. In addition, any initial differences between the two populations decays, and is replaced by a strong sub-Poissonian correlation. This is due to the fact that all births must occur in a way that tends to equalize the two species that are present.

## B. Means and correlations

To calculate analytic solutions, standard Ito calculus can be used to obtain the exact time-evolution of correlations and expectation values. This is straightforward, since in Ito calculus the noise terms are not correlated with the other stochastic variables at the same time, so  $\text{h}f(\alpha_i)\zeta_j(t) = 0$ . Thus, the means and variances are all soluble from their respective time-evolution equations - which is also possible using the master-equation form. Defining the initial means and correlations as:  $\overline{n_+} = \ln_+(0)$ ,  $\overline{n} = \ln(0)$ ,  $\overline{n_+^2} = \ln_+^2(0)$ ,  $\overline{n^2} = \ln^2(0)$  and  $\overline{n_+ n} = \ln_+(0)n(0)$ , one directly obtains the following exact results:

$$\begin{aligned}\ln_+(t) &= \overline{n_+} e^{k t} \\ \ln(t) &= \overline{n} e^{k^* t} \\ \ln_+^2(t) &= \overline{n_+^2} e^{2k t} + 2k_m e^{3k t} \frac{\sinh(k t/2)}{k/2} \\ \ln^2(t) &= \overline{n^2} e^{2k^* t} + \frac{2k_m \overline{n_+}}{k + 3k_m} e^{k t} e^{2k^* t} \\ \ln_+(t)n(t) &= \overline{n_+ n} e^{2kt} : \quad (5.6)\end{aligned}$$

Suppose that  $k_m = k$ , so the mean population is time-invariant. Then the asymptotic population differences have a mean and variance of:

$$\begin{aligned}\lim_{t \rightarrow \infty} \ln_+(t) &= 0 \\ \lim_{t \rightarrow \infty} \ln_+(t)^2 &= \lim_{t \rightarrow \infty} \ln(t)^2 + n_+(t) \\ &= \frac{\overline{n_+}}{2} : \quad (5.7)\end{aligned}$$

This indicates that the population difference has a steady-state variance of half its usual value, owing to the fact that all births are correlated between the species, thus causing sub-Poissonian statistics - while all deaths are uncorrelated, thus tending to restore the Poissonian distribution. By comparison, the variance in the total population shows linear growth

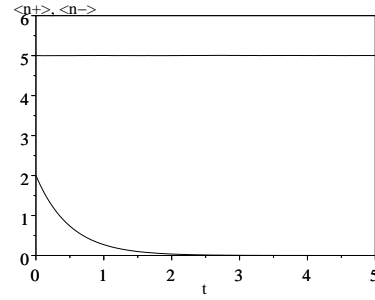


Figure 1: Sampled moments of  $\ln_+$  (upper curve) and  $\ln$  (lower curve) for genetic mutation example in the Poisson representation, parameters as in text. Sampling error ( $\sigma_m$ ) is of order  $10^{-3}$  or less.

in this case, as some populations in the total ensemble become extinct, while others can randomly grow to a large population.

In this case there are no unstable trajectories, and the positive Poisson method can be used with zero gauge terms. However, it should be noted that this model is rather simple, ignoring competition between the two species: which could lead to nonlinear effects requiring gauge corrections.

## C. Numerical results

Applying the Stratonovic rules to generate equations for integration results in:

$$\begin{aligned}\frac{dn_+}{dt} &= k_m = 2 - k n_+ + \frac{p}{2k_m n_+} \zeta_1(t) \\ \frac{dn}{dt} &= k^* n + i \frac{p}{2k_m n_+} \zeta_2(t) : \quad (5.8)\end{aligned}$$

This illustrates the typical feature of the Stratonovic calculus, which is the generation of terms in the drift equations due to the noise. Some care is needed in calculations near the absorbing boundary at  $n_+ = 0$ , which is treated by imposing an appropriate boundary condition at this point.

Fig (1) shows the mean values obtained from numerical simulation of these equations for an ensemble of  $10^6$  trajectories. The numerical and analytic results are indistinguishable at this graphic resolution.

The results for population variances and cross-correlations are shown in Fig (2), also agreeing extremely well with the analytic predictions.

The integrations were for a total time of  $t = 5$ , using values of  $k = k_m = 1$ . The minimum step-sizes used were  $\Delta t = 0.01$  and  $\Delta t = 0.005$ . Initial values were set to  $n_+ = 5$ ,  $n = 2$ , to give results in low population regions with large departures from Poissonian behavior. All simulation results agree well within the sampling error, as shown in the Table (1) - except for the result for  $\ln$ , where the residual discrepancy of  $10^{-8}$  is actually caused by a small discretization error of  $\sim 2 \cdot 10^{-8}$ , since the sampling error is zero in this quantity.

In summary, for this example, all the simulation results are in excellent agreement with analytic predictions for this

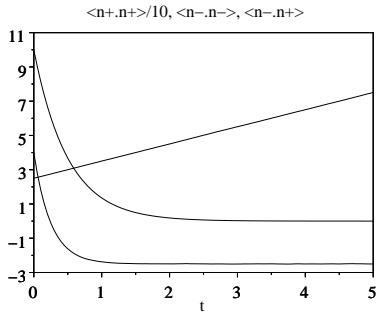


Figure 2: Sampled moments of  $hn_i^2$  ( $i=10$  (straight line),  $hn_i n_i$  (middle curve) and  $hn^2 i$  (lowest curve), for genetic mutation example in the Poisson representation, parameters as in text. Sampling error is of order  $10^{-3}$  or less.

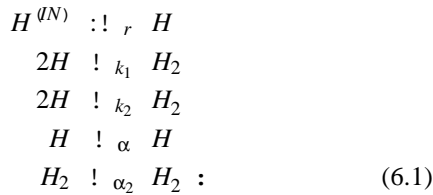
Moment	Analytic	Poisson
$hn_i i$	5.0	5.002 (7)
$hn_i$	$0.9080 \cdot 10^{-4}$	$0.9079(0) \cdot 10^{-4}$
$hn_i^2 i$	75	75.1 (2)
$hn^2 i$	25	25.02 (7)
$hn_i n_i$	$0.4540 \cdot 10^{-3}$	$0.4541(6) \cdot 10^{-3}$

Table I: Table of observed moments (standard deviations  $\sigma_m$  in brackets), comparing analytic and simulated results for the genetic equations in the Poisson expansion at  $t = 5$ .

model.

## VI. ASTROPHYSICAL MOLECULAR HYDROGEN PRODUCTION

The previous results do not yet involve stochastic gauges. These are only needed when the equations are nonlinear, which comes about when multi-component competition or formation processes are present. To give a typical example of this, consider the astrophysically important problem of hydrogen recombination to form molecules on interstellar grain surfaces[5]. This is thought to be the major source of interstellar  $H_2$ , and it is known that conventional rate equations are unable to describe this accurately, due to low occupation numbers at the critical step of dimer formation. The main reactions are:



This describes a species  $H$  which can grow via a generation rate ( $r$ ) from an input flux  $H^{(IN)}$ , until it reaches an equilibrium[1] due to losses from molecule formation ( $k = k_1 + k_2$ ), and desorption ( $\alpha$ ), which stabilizes the concentration of  $H$ . The concentration of  $H_2$  is also stabilized by des-

orption ( $\alpha_2$ ). There are additional effects due to flux-blocking of  $r$  caused by adsorbed molecules and atoms, which are described by extra terms  $k_5$  and  $k_6$  that are negligible at low fluxes.

### A. Analytic solutions

We can introduce Poisson variables  $\alpha_1; \alpha_2; \alpha_3; \alpha_4$ , representing  $[H]; [H_2]; [H]; [H_2]$  respectively, and define  $n = \alpha_1$ , which is the hydrogen atom number. From the Poisson expansion viewpoint, the only non-trivial term is the hydrogen equation, as this introduces noise. The resulting Fokker-Planck equation is simply:

$$\frac{\partial}{\partial t} G(n; t) = \frac{\partial}{\partial n} (r + \gamma n + 2kn^2) - k \frac{\partial}{\partial n^2} n^2 G(n; t) : \quad (6.2)$$

This has a steady-state which is exactly soluble, though defined on a complex contour starting and ending at the origin:

$$G(n; \infty) = C n^{\gamma-k/2} \exp(-2n + \frac{r}{kn}) : \quad (6.3)$$

Here I have kept the derivatives in analytic form, to obtain the simplest potential solution. However, the result is instructive, since it is clear that this analytic form is inherently complex. This is the essential reason why a gauge variable  $\Omega$  is needed in order to get simulations that behave like this simple, compact solution. The gauge variable can attain complex values during a stochastic calculation, even when the distribution itself is constrained to have positive values

For simplicity, I introduce relative flux and relaxation parameters,  $\varepsilon = r/\Omega k$  and  $\nu = \alpha/2k$ . Next, using a Sommerfeld contour-integral identity in the inverse variable  $\mu = 1/n$  - one obtains the result that:

$$\begin{aligned}
 n^M &= C \int_{-\infty}^{0+} \mu^{\Omega - M/2\nu} e^{2\varepsilon(\mu + 1/\varepsilon\mu))} d\mu \\
 &= \varepsilon^{M/2} I_{2\nu+M-1}(\frac{r}{\varepsilon}) = I_{2\nu-1}(\frac{r}{\varepsilon}) :
 \end{aligned} \quad (6.4)$$

This exact solution gives the  $H_2$  production rate (neglecting dissociation):  $R_{H_2} = k hn_i = n^2$ .

An obvious result, coming from the asymptotic properties of Bessel functions, is that

$$\begin{aligned}
 \lim_{\varepsilon \rightarrow \infty} n^M &= \varepsilon^{M/2} ; \\
 \lim_{\varepsilon \rightarrow 0} n^M &= \frac{r^M}{(\gamma + k[M-1])} :: (\alpha)
 \end{aligned} \quad (6.5)$$

Thus for large grains with  $\varepsilon \rightarrow \infty$  the high flux limit is just  $R_{H_2} = k\varepsilon$ , which is also the rate-equation limit. At low fluxes (i.e., small grains) a dramatic and physically understandable feature is obtained: the  $H_2$  production rate can be suppressed below the rate equation result. In this limit of  $\varepsilon \rightarrow 0$ ,

$$\begin{aligned}
 hn_i &= \frac{r}{\gamma} \\
 n^2 &= \frac{r^2}{\gamma(k + \gamma)} :
 \end{aligned} \quad (6.6)$$

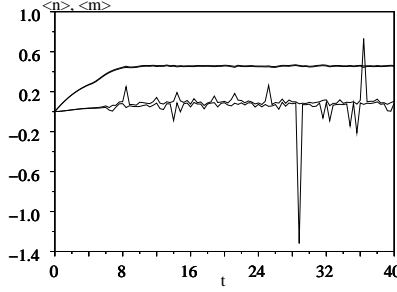


Figure 3: Sampled moments of  $hni$  (upper curve) and  $hni = hn^2i$  (lower curve) for astrophysical hydrogen molecule production in the Poisson representation, parameters as in text. Adjacent lines give upper and lower ( $\sigma_m$ ) error bounds caused by sampling error.

For  $k = \gamma$ , this predicts enormously reduced hydrogen molecule production rates compared to normal rate equations. The reason for this is simply that when there is only one atom at a time on the grain, no molecules are produced. This result has been found in earlier Monte Carlo calculations as well[5], so it is a verification of the current procedures to reproduce this known result.

### B. Stochastic equations

It is simplest to use a scaled time  $\tau = 2kt$  to calculate the stochastic equations in  $n$ . With this variable the drift and noise matrices are both scalars. The resulting Ito stochastic equations, including the gauge terms for astrophysical hydrogen production, are:

$$\begin{aligned} \frac{d\Omega}{dt} &= \Omega g \zeta \\ \frac{dn}{dt} &= \epsilon \nabla n \cdot \vec{n} + in \zeta \quad g : \end{aligned} \quad (6.7)$$

These equations are unstable in the absence of gauge terms. There is a singular trajectory  $n \rightarrow -\infty$  which can be accessed via the complex diffusion of  $n$  into the negative half-space of  $n < 0$ . Previous work on similar equations in quantum optics[8, 9] has shown that this leads to systematic errors, due to the resulting power-law tails in the distribution, which can introduce boundary terms if Eq. (2.6) is integrated by parts directly.

Results of the numerical simulations in the Poisson representation, showing upper and lower one-standard deviation error-curves, are given in Fig (3). The results clearly show the problems caused by the dynamical instabilities in these equations, which cause both a large sampling error, and systematic errors. These equations are exceptionally difficult to integrate numerically, owing to the instabilities, and it is essential to integrate by alternating between  $n$  (for  $|n| < 1$ , and  $1=n$  (for  $|n| > 1$ ) in order to obtain stable numerical results.

Numerical results throughout this section were obtained using parameters of  $\epsilon = 0.1$ ,  $v = 0.1$  for which the analytic re-

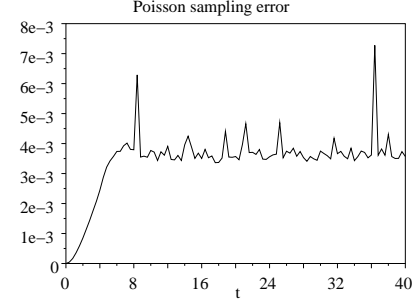


Figure 4: Standard deviation  $\sigma_m$  in the mean  $hni$  for astrophysical hydrogen in the Poisson representation.

sults can be easily calculated from the Bessel function representation. In this region the rate equations break down, and occupation numbers are very small, which is a testing region of parameter space for these expansions - since the fluctuations are far from Poissonian. The integrations were for a total time of  $\tau = t = 40$  to allow an approximate numerical steady-state to be reached from an initial value of  $n = 0$  (for simplicity, a value of  $k = 1=2$  was taken). The minimum step-sizes used were  $\Delta t = 0.005$  and  $\Delta \tau = 0.0025$ .

While the sampling error in the molecule production rate is large, the sampling error in the atom number is relatively stable in time. A graph of this quantity is provided in Fig (4). The fact that this does not grow in time indicates that the distribution has equilibrated, although the discrepancy between these results and the exact ones indicates that the apparent equilibrium does not correspond to a solution of the master equation.

### C. Stabilizing gauges

Fortunately, it is simple to stabilize these equations by adding non-analytic corrections to the drift. For example, consider the effects of three different gauges which all stabilize the equations:

$$\begin{aligned} g_c &= i(n - \bar{n}) \quad [circular] \\ g_p &= i(x - \bar{x}) \quad [phase] \\ g_s &= 2ix\theta(x) \quad [step]: \end{aligned} \quad (6.8)$$

In the minimal circular gauge, the Stratonovic equations are:

$$\begin{aligned} \frac{d\Omega}{d\tau} &= \Omega g_c \zeta + (n - \bar{n})^2 = 2 \\ \frac{dn}{d\tau} &= \epsilon \nabla n \cdot \vec{v} - 1=2 + j_t \zeta + in\zeta : \end{aligned} \quad (6.9)$$

In the phase gauge, the Stratonovic equations are:

$$\begin{aligned} \frac{d\Omega}{d\tau} &= \Omega g_p \zeta + (i y - \bar{y})^2 = 2 \\ \frac{dn}{d\tau} &= \epsilon \nabla n \cdot \vec{v} - 1=2 + j_t \zeta + iy + in\zeta : \end{aligned} \quad (6.10)$$

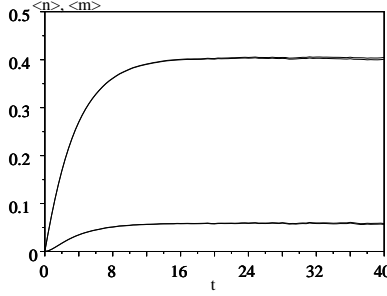


Figure 5: Sampled moments of  $hni$  (upper curve) and  $hni = hn^2 i$  (lower curve) for astrophysical hydrogen molecule production in the ‘phase’ gauge, parameters as in text. Adjacent lines give upper and lower ( $\sigma_m$ ) error bounds caused by sampling error.

In the step gauge, the equations are coordinate dependent:

$$\begin{aligned} \frac{d\Omega}{d\tau} &= \Omega g_s \zeta + iy \quad g_s^2 = 2 \quad (x < 0) \\ \frac{dn}{d\tau} &= \varepsilon n [v - 1/2 - n] + in\zeta \quad (x < 0) : \\ &= \varepsilon n [v - 1/2 + n] + in\zeta \quad (x > 0) : \end{aligned} \quad (6.11)$$

Clearly the first two equations only have inward drift vectors with  $d\mathbf{p}/dt < 0$  at large enough  $|\mathbf{p}|$ . The last, the step gauge, is similar, except that it shows linear growth if  $v < 1/2$  and  $x = 0$ . At worst this can only lead to a singularity in infinite time, and in any event the  $y$ -axis is not an attractor: so growth along the  $y$  axis only leads to a temporary increase in radius, not a singularity. Hence, all three gauges are completely stable, with no moving singularities.

#### D. Numerical simulations

As results in all three gauges were similar, apart from changes to the sampling error, I will only show graphs of the detailed results in the phase-stabilized gauge.

Results of the numerical simulations in the phase-stabilized gauge, showing upper and lower one-standard deviation error-curves, are given in Fig (5). It is clearly dramatically improved compared to the Poisson results.

While the sampling error is growing in time as shown in Fig (6), it is scarcely visible on the mean value graphs - with improvements of up to three orders of magnitude in the sampling error of molecule production rates, relative to the Poisson method.

#### E. Comparison of moments and sampling errors

Apart from the unmodified Poisson or ‘zero gauge’ results, the gauge simulations are stable. Nevertheless, on closer inspection, the stable gauges don’t behave in an identical way as regards the sampling error with a finite set of trajectories.

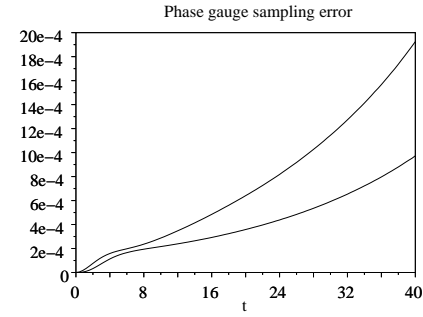


Figure 6: Sampling error standard deviation  $\sigma_m$  in the mean  $hni$  (upper curve) and in  $hni = hn^2 i$  (lower curve) for astrophysical hydrogen in the phase gauge.

Moment	Analytic	Poisson	Circular	Phase	Step
$h\Omega i$	1.0	1.0	0.994 (10)	0.997 (4)	1.005 (6)
$hni$	0.407 ::	0.457 (4)	0.402 (5)	0.403 (2)	0.406 (4)
$hni = hn^2 i$	0.059 ::	0.094 (8)	0.061 (2)	0.057 (1)	0.064 (3)

Table II: Table of observed moments, comparing analytic and simulated results for three different stochastic gauges and the Poisson expansion; the moment  $hni = hn^2 i$  is critical for molecule production. Sampling error ( $\sigma_m$ ) in brackets.

For each gauge and for the Poisson expansion, the observed moment and its sampling error  $\sigma_m$  (standard deviation in the mean) is given in Table 2, which tabulates the final near-equilibrium simulation results at  $t = 40$ , and compares them to the equilibrium analytic result for  $t = \infty$ . For the stable gauges, the results are within  $\sigma_m$  of the analytic calculations in most cases, and are within  $2\sigma_m$  in the remaining more accurate cases - where the residual discrepancy was partly due to the finite time-step discretization error. This indicates that all these (stable) gauges converge to the analytically known correct answer.

The corresponding (unstable) Poisson method clearly gives incorrect answers due to systematic boundary term errors, with up to  $12\sigma_m$  discrepancy in the case of the mean number of hydrogen atoms,  $hni$ . The graphical and tabular evidence indicates that the mean atom number is incorrect because the unstable trajectories cause power-law tails in the distribution, and consequent boundary term errors. In addition, the graph shows that the Poisson time-history has large fluctuations, showing no signs of equilibration for the molecule number  $hni$ . This is further evidence for power-law tails, which are also found in a similar quantum-optical master equation.

The circular gauge has no systematic errors, but gives the worst sampling error of the stable gauges, as the  $n$  variable is the least constrained in this gauge, tending to diffuse in a circle. For these parameters the phase gauge gives the best results, as it localizes the  $n$  variable near a deterministic stable point. The last gauge is a step gauge - only giving non-zero corrections when  $x < 0$ . This has the feature that the gauge term  $\Omega$  only changes when the trajectory has the (unusual) value of  $x < 0$ , and gives sampling errors intermediate

between the other two.

One might have expected that the step gauge would give lower gauge noise errors, possibly with a smaller standard deviation in  $\hbar\Omega_i$ , since this gauge is zero in the right half-plane. Instead, the phase-stabilized gauge gives the lowest overall sampling errors for all quantities with these parameter values, even for the gauge amplitude  $\hbar\Omega_i$ . Presumably this result is an example of ‘prevention is better than cure’. That is, phase-stabilization is also able to prevent amplitudes from growing along the  $y$  axis. The step gauge corrects this growth too late for optimal results, having to use a numerically bigger gauge correction with larger sampling errors.

## VII. CONCLUSION

The gauge Poisson method is shown to generate a stochastic differential equation that is exactly equivalent to a master equation. This provides a complete solution to the problem of stochastic equivalence of kinetic master equations - which has not been treated in full previously. By comparison, the system-size expansion is only approximate, and the positive Poisson representation is not exact for problems which have boundary terms due to moving singularities. The gauge technique provides a way to eliminate any boundary-term errors due to singular trajectories, although the price paid for this advantage is an extra stochastic gauge amplitude, which generates a sampling error that grows in time. The focus of numerical simulations in this paper is on cases where the existence of exact analytic results allows the issue of random and systematic errors to be carefully investigated.

It should be remarked that this type of model is very general. For example, one can easily include linear diffusion and extend the theory to treat fluctuations in reaction-diffusion models or even Boltzmann kinetics[3]. This simply requires that the populations are defined as occurring in a lattice of

bounded cells, either in ordinary space or in a classical phase-space, together with the appropriate hopping rates. This simplicity is a great advantage of Poisson-based expansions, as compared to direct Monte-Carlo simulations. The relevant linear deterministic equations are just the same as would occur in discretized non-stochastic equations. However, one finds that it becomes necessary to include cell-volume factors in the nonlinear rate constants, so that the noise terms vary with the  $j$  th lattice cell volume  $V_j$  - typically resulting in stochastic noise terms proportional to  $1 = \sqrt{V_j}$ . Applications to these problems will be treated elsewhere.

The technique can be easily extended to include a large number of coupled kinetic processes, as occurs both in genetics, and in the generation of chemical species of astrophysical importance: for example,  $OH; H_2O$ ,  $CO$  and so on. By contrast, the direct solution of the master equation grows exponentially more complex as the number of interacting species increases. Similar considerations arise when treating biological species with typically very large numbers of genotypes, or when treating extended spatial (multi-mode) problems. The method of choosing generically stable gauges developed here may also be in some degree useful for the corresponding quantum problems.

## Acknowledgments

Numerical calculations were carried out using open software from the XMDS project[15]. Thanks to the Australian Research Council and the Alexander von Humboldt-Stiftung for providing research support. Useful discussions on genetic models with A. Drummond (Oxford) and on astrophysical models with O. Biham (Jerusalem) are gratefully acknowledged.

---

[1] H. Haken, *Synergetics: An Introduction* (2nd Ed, Springer, Berlin, Heidelberg, New York, 1978).

[2] N. G. Van Kampen, *Stochastic processes in Physics and Chemistry* (North-Holland, Amsterdam, 1992).

[3] I. Matheson, D. F. Walls, C. W. Gardiner, *J. Stat. Phys* **12**, 21 (1975); C.W. Gardiner, S. Chaturvedi, *J. Stat. Phys.* **17**, 429 (1977); **18**, 501 (1978); C. W. Gardiner, *Handbook of Stochastic Methods*, (2nd Ed, Springer, Berlin, Heidelberg, New York, 1985).

[4] M. Eigen, *Naturwissenschaften* **58**, 465 (1971); I. Hanski, *Nature* **396**, 41 (1998); D. Alves and J. F. Fontanari, *Phys. Rev E* **57**, 7008 (1998); B. Drossel, *Advances in Physics* **50**, 209 (2001).

[5] S. B. Charnley, *Astrophys J* **509**, L121 (1998); *Astrophys J* **562**, L99 (2001); O. Biham, I. Furman, V. Pirronello and G. Vidali, *Astrophys. J.* **553**, 595 (2001).

[6] D. T. Gillespie, *J. Comput. Phys.* **22**, 403 (1976); *J. Chem. Phys* **81**, 2340 (1977).

[7] S. Chaturvedi, P. D. Drummond and D. F. Walls, *J. Phys. A* **10**, L187-192 (1977); P. D. Drummond and C. W. Gardiner, *J. Phys. A* **13**, 2353 (1980).

[8] A. M. Smith and C. W. Gardiner, *Phys. Rev. A* **39**, 3511 (1989); R. Schack and A. Schenzle, *Phys. Rev. A* **44**, 682 (1991).

[9] A. Gilchrist, C. W. Gardiner, and P. D. Drummond, *Phys. Rev. A* **55**, 3014 (1997).

[10] P. Deuar and P. D. Drummond, *Comp. Phys. Comm.* **142**, 442 (2001); I. Carusotto, Y. Castin and J. Dalibard, *Phys. Rev. A* **63**, 023606 (2001).

[11] P. Deuar and P. D. Drummond, *Phys. Rev. A* **66**, 033812 (2002).

[12] A. Ramani, B. Grammaticos, and T. Bountis, *Physics Reports* **180**, 159 (1989).

[13] F. Baras and M. Malek Mansour, *Phys. Rev. E* **54**, 6139, (1996); U. L. Fulco, D. N. Messias, M. L. Lyra, *Phys. Rev. E* **63**, 066118 (2001).

[14] P. D. Drummond and I. K. Mortimer, *J. Comp. Phys.* **93**, 144-170 (1991).

[15] G. R. Collecutt, P. D. Drummond, *Comput. Phys. Commun.* **142**, 219-223 (2001); <http://www.physics.uq.edu.au/xmds/>